Vol. 85 (1994) *ACTA PHYSICA POLONICA A* No. 1

Proceedings of the European Conference "Physics of Magnetism 93", Poznań 1993

PHASE STRUCTURE IN Fe–Cr–Co PERMANENT MAGNET ALLOY

J. OLSZEWSKI, S. SZYMURA, J. WÓJCIK AND B. WYSŁOCKI

Institute of Physics, Technical University of Częstochowa
Armii Krajowej 19, 42-200 Częstochowa, Poland

The Mössbauer spectroscopy, electron microscopy and magnetization measurements were used in order to describe structural changes in $Fe_{58.75}Cr_{29.4}Co_{11.85}$ alloy during magnetic hardening. Multiphase structure was found in alloy with best magnetic properties.

PACS numbers: 75.60.Gm, 75.60.Ej

1. Introduction

Fe–Cr–Co alloys are well known as hard magnetic materials with good mechanical workability [1]. The mechanism of the magnetic hardening in these alloys is usually attributed to spinodal decomposition of supersaturated solution based on α-Fe into two isomorphous phases (Fe–Co-rich ferromagnetic (α_1) and Cr-rich weakly ferromagnetic or paramagnetic (α_2) phase)(see as an example [2]). The microstructure of these alloys is usually characterized as the single-domain precipitations of the α_1 phase embedded in α_2 matrix (see as an example [3]). The aim of this paper is more detailed description of phase changes in the $Fe_{58.75}Cr_{29.4}Co_{11.85}$ alloy during thermomagnetic treatment (TMT).

2. Experiment

The $Fe_{58.75}Cr_{29.4}Co_{11.85}$ alloy was prepared by induction melting together electrolytic Fe, Cr, Co and thermomagnetically treated to achieve hard magnetic state. Following TMT was applied: ageing at 1570 K for 1 h and ice-water quenching (A), cooling from 970 to 890 K at the rate 60 K/h in external magnetic field $H = 300$ kA/m (B), holding in 880 K for 2 h (C), cooling from 870 K to 820 K (D) and then to 770 K (E) at the rate 10 K/h, ageing at 770 K for 12 h (F) and for 150 h (G).

After each stage of TMT (A–G) the magnetic properties such as: coercivity (H_c), residual magnetization (M_r) and saturation magnetization (M_s) were measured using DC hysteresigraph. Simultaneously, the phase structure was analyzed by electron microscopy (for stage F and G) and the Mössbauer transmission spectroscopy. The Mössbauer spectra were computer analyzed using Hesse–Rubartsch's

method for determination of the magnetic hyperfine field distribution ($P(B)$), and by the least squares fitting program assuming Lorentzian lines. All measurements were performed at room temperature.

3. Results and discussion

Representative $P(B)$ curves and magnetic properties of the investigated alloy after each stage of the TMT are shown in Fig. 1 and Table I, respectively.

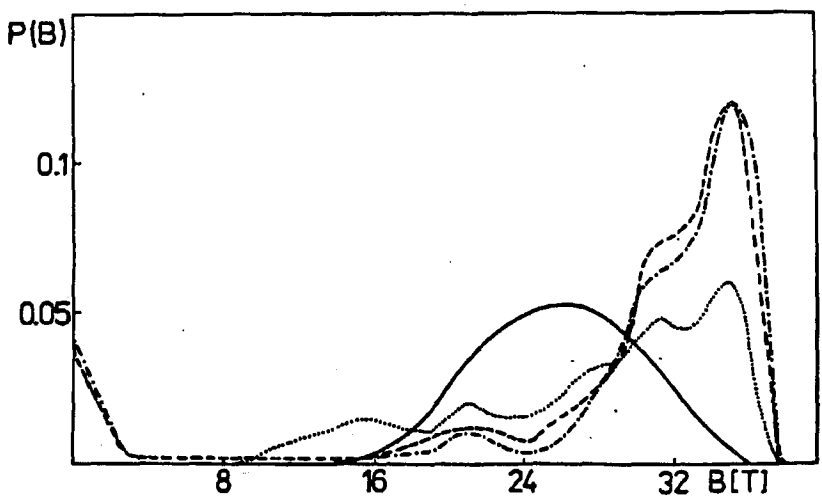

Fig. 1. Magnetic hyperfine field distribution for the $Fe_{58.75}Cr_{29.4}Co_{11.85}$ alloy after different stages of TMT: stage A (——), stage B (· · · · ·), stage F (– · – · – ·), stage G (– – – –).

As can be seen from Fig. 1 (solid line) $P(B)$ curve for the $Fe_{58.75}Cr_{29.4}Co_{11.85}$ alloy has Gaussian-like shape (with isomer shift (IS) −0.02 mm/s) which points out that the alloy has monophase structure. However, after cooling in external magnetic field $P(B)$ curve for this alloy can be decomposed into five components (first with B_{eff} = 35.2 T and IS = 0.02 mm/s, second with B_{eff} = 31.7 T and IS = 0.007 mm/s, third with B_{eff} = 28.2 T and IS = −0.007 mm/s, fourth with B_{eff} = 20.8 T and IS = −0.035 mm/s, fifth with B_{eff} = 16.0 T and IS = −0.053 mm/s) (Fig. 1, dotted line). It indicates that alloy can be represented by five areas with different environments of Fe atoms. Values of B_{eff} and IS of each elementary Zeeman spectrum do not vary, only their intensities change during TMT. The fifth sextet vanishes during the stage C and at the same time paramagnetic peak with IS = −0.114 mm/s appears. Turning to account data from [4, 5], the sextets could be identified as coming from Fe_7Co_1, $Fe_6Co_1Cr_1$, $Fe_5Co_1Cr_2$,

$Fe_3Co_1Cr_4$, $(Fe_xCo_{1-x})_{40}Cr_{60}$ phase and the single line from $(Fe_xCo_{1-x})_{25}Cr_{75}$ phase. Volume fractions of each phase, after each step of TMT, are shown in Table II.

TABLE I

Magnetic properties of the $Fe_{58.75}Cr_{29.4}Co_{11.85}$ alloy after each stage of thermomagnetic treatment.

Stage of TMT	M_s [T]	M_r/M_s	H_c [kA/m]
B	1.54	0.4	2.7
C	1.54	0.6	7.6
D	1.50	0.72	20.6
E	1.47	0.89	42.0
F	1.45	0.905	45.5
G	1.45	0.89	43.5

TABLE II

Volume fractions of precipitated phases in the $Fe_{58.75}Cr_{29.4}Co_{11.85}$ alloy after each stage of thermomagnetic treatment.

	Stage of TMT					
	B	*C*	*D*	*E*	*F*	*G*
Fe_7Co_1	0.13	0.16	0.20	0.27	0.29	0.29
$Fe_6Co_1Cr_1$	0.23	0.24	0.26	0.23	0.24	0.23
$Fe_5Co_1Cr_2$	0.22	0.19	0.17	0.14	0.11	0.13
$Fe_3Co_1Cr_4$	0.21	0.22	0.20	0.14	0.11	0.14
$(Fe_xCo_{1-x})_{40}Cr_{60}$	0.21	0.19	–	–	–	–
$(Fe_xCo_{1-x})_{25}Cr_{75}$	–	–	0.17	0.22	0.25	0.21

As can be seen from Table I, the $Fe_{58.75}Cr_{29.4}Co_{11.85}$ alloy has best hard magnetic properties after *F* stage of TMT, when it consists of four ferromagnetic and one paramagnetic phases occupying respectively 75% and 25% of total volume (Table II). Micrographs taken from this alloy on the same stage of TMT show rod-like or rectangular parallelepiped precipitations of ferromagnetic phases separated from each other by paramagnetic matrix. Average diameter of ferromagnetic particles is about 40 nm and average length about 240 nm. Therefore, they can be treated as single-domain ones.

After prolonged aging (stage G of TMT) H_c and M_r decreased. It seems to be connected with the fact that volume fraction of paramagnetic phase decreases, ferromagnetic particles grow and aggregate. Therefore, magnetization reversal process can occur at lower external field by movement of domain walls.

Summarizing our discussion, we can tell that phase structure of the $Fe_{58.75}Cr_{29.4}Co_{11.85}$ alloy is more complicated than that usually described. Ferromagnetic particles in hard magnetic state consist of four well defined regions with different chemical compositions. Magnetic properties of this alloy depend on volume fractions of each phase and their arrangement.

References

[1] H. Kaneko, M. Homma, K. Nakamura, *AIP Conf. Proc.* **5**, 1088 (1971).

[2] R. Tahara, Y. Nakamura, M. Inagaki, Y. Iwama, *Phys. Status Solidi A* **41**, 451 (1977).

[3] M. Okada, G. Thomas, M. Homma, H. Kaneko, *IEEE Trans. Magn.* **MAG-14**, 245 (1978).

[4] L. Schwartz, D. Chandro, *Phys. Status Solidi B* **45**, 201 (1977).

[5] B. De Mayo, D.W. Ferster, S. Spooner, *J. Appl. Phys.* **41**, 1319 (1970).